

Operating a Multi-Level Molecular Dimer Switch through Precise Tip-Molecule Control

Yueqing Shi^{1,*}, Weike Quan^{1,2,*}, Liya Bi^{1,2}, Zihao Wang^{1,2}, Kangkai Liang^{1,2}, Hao Zhou¹, Zhiyuan

Yin¹, Wan-Lu Li^{2,3} and Shaowei Li^{1,2,†}

¹ Department of Chemistry and Biochemistry, University of California, San Diego, La Jolla, CA 92093-0309, USA

² Program in Materials Science and Engineering, University of California, San Diego, La Jolla, CA 92093-0418, USA

³ Aiiso Yufeng Li Family Department of Chemical and Nano Engineering, University of California, San Diego, La Jolla, CA 92093-0448, USA

Abstract

Controlling structural transitions between molecular configurations is crucial for advancing functional molecular electronics. While reversible switching of bistable two-state molecules has been achieved, creating molecular systems that can be controllably switched between multiple configurations often requires complex synthetic methods, presenting a much greater challenge. In this study, we showcase a straightforward yet effective strategy to create and control transitions between multiple molecular structural states by forming a surface-bound molecular dimer. Using low-temperature scanning tunneling microscopy, we induce and characterize the structural transitions of a pyrrolidine dimer on a Cu(100) surface. The intermolecular interactions open new energy transfer channels, enabling the excitation through pathways that were inaccessible in monomers. The occupation of different molecular states is highly sensitive to both the energy of the tunneling electrons and the interaction with the STM tip. By precisely adjusting the tip-molecule distance, we can select the most probable structural configuration based on sample bias, thereby achieving on-demand control of this molecular dimer switch. This work highlights an approach that leverages both intermolecular and molecule-environment interactions to create and control an artificially fabricated molecular device.

* These authors contribute equally to this work.

† Corresponding information: shaoweili@ucsd.edu

Introduction

Molecular electronics is a promising frontier for developing alternatives to traditional silicon-based technologies¹⁻⁵. Precise control over transitions between molecular structural⁶⁻¹⁰, electronic¹¹⁻¹³, or spin^{14, 15} states offers a range of strategies for realizing various molecular fundamental devices¹⁶⁻¹⁹. Among these approaches, exploiting molecular structural transitions, where molecules switch between two or more stable configurations, has shown potential as a key component in applications such as data storage and logic gates²⁰⁻²⁴. While reversible transitions between bistable two-state molecular systems — such as proton transfer^{25, 26}, cis-trans transition²⁷⁻³⁰, and ring opening/closing^{31, 32} — occur naturally across various molecular systems, materials that can switch between multiple stable configurations are rare in nature. Designing and synthesizing the candidates of a multi-level molecular switch remains a significant challenge due to the complexity of creating molecules with the desired structures.

Scanning tunneling microscopy (STM) has become an indispensable tool for developing single-molecule functional devices because of its ability to resolve, characterize, and manipulate surface-adsorbed molecules with sub-angstrom precision. STM's high spatial resolution enables the detection of the changes in molecular states arising from various processes such as physical actions^{10, 33-35}, tautomerization^{16, 26, 36}, and other dynamic reactions^{37, 38}. Additionally, STM can deliver external stimuli, either by injecting energetic tunneling electrons^{39, 40} or by applying external forces through the tip^{10, 41-43}, to precisely excite the transition of the single molecule in the STM junction. More importantly, STM can manipulate surface adsorbates to create artificial structures, enabling the atomic-scale synthesis of molecular clusters with functionalities that individual molecules do not possess.

In this study, we demonstrate the controlled switching between multiple structural states of an artificially fabricated molecular dimer. Individual pyrrolidine molecules adsorbed on Cu(100) can be manipulated into dimers with a specific separation. We utilize STM to induce and control the transitions between various configurations of this pyrrolidine dimer. Our findings reveal that this pair of molecules can adopt six distinct configurational states, which can be switched from one to another when excited by tunneling electrons. Intermolecular interactions enable energy transfer between the two molecules, allowing excitation through pathways not accessible in monomers. By harnessing both intermolecular coupling and tip-molecule interactions, we were able to distinguish and control these molecular states through precise tuning of the tunneling electron energy and tip-molecule distance.

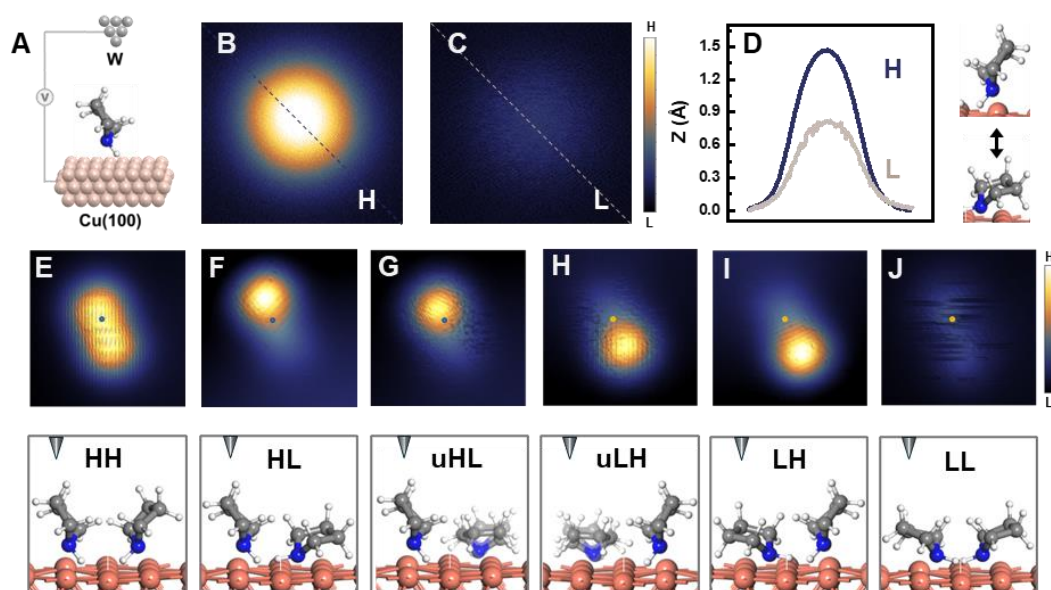


Figure 1. Multiple structural states of pyrrolidine monomer and dimer on the Cu(100) surface. (A) Schematic diagram of a pyrrolidine monomer adsorbed on Cu(100) probed with STM. (B)-(C) Topographic images revealing the High (B) and Low (C) states of pyrrolidine monomer. Image scale: $1.3 \text{ nm} \times 1.3 \text{ nm}$. (D) Line-cut profiles of the two states along the dashed line in (B) and (C). The monomer can reversibly switch between these two states when excited by tunneling electrons. (E)-(J) Topographic images revealing the six structural states of a pyrrolidine dimer. Image scale: $1.4 \text{ nm} \times 1.4 \text{ nm}$. (E) High-High (HH) state, (F) Stable High-Low (HL) state, (G) Unstable High-Low (uHL) state, (H) Unstable Low-High (uLH) state, (I) Stable Low-High (LH) state, (J) Low-Low (LL) state. The circle indicates where the tip is positioned to record the current-time trace. The tunneling gap was set at 50 mV sample bias, 20 pA tunneling current, with the feedback on for Figure (B)-(C), and with the feedback off for Figure (E)-(J).

Results and Discussion

The building block of our multi-level molecular switch is the single pyrrolidine molecules, characterized by its simple five-membered saturated ring consisting of one nitrogen and four carbon atoms (**Figure 1A**). The pyrrolidine monomer is known to have two distinct structural conformations when adsorbed on Cu(100), standing and bent toward the surface, namely the high (H) state and the low (L) state, which are associated with varying apparent heights as depicted in **Figure 1B-D**. Existing reports indicate that the excitation of specific vibrational modes by inelastic tunneling electrons enables the pyrrolidine monomer to reversibly transition between these two structures^{44, 45}, serving as a simple example of a bi-level molecular switch. When adsorbed on the four-fold symmetric Cu(100) surface, pyrrolidine molecules exhibit rapid reversible rotation among four equivalent orientations, resulting in a circular appearance in both high and low states.

Pyrrolidine dimers can be formed naturally at a relatively high molecular coverage or through artificial manipulation with the STM tip following established techniques⁴⁶⁻⁴⁸. On the Cu(100) surface, pyrrolidines can be arranged into pairs with varying intermolecular distances. When two molecules are relatively far apart, each molecule switches independently, showing no significant correlation. However, when two molecules become closely packed, they form a single, stable configuration that is unable to change further. In the specific type of dimer with intermolecular separation of 0.4 nm investigated in this study, we observed six distinct states in both topographic images and tunneling current traces — exceeding the four states expected from the simple combinations of the two states of each monomer. Besides both molecules in the high state (HH), and both in the low state (LL), we find two pairs, four possible states corresponding to one molecule in the high state and the other in the low state. One pair shows relatively scraping signals in the topographic image (**Figure 1G and 1H**), making it appear less stable. They are referred to as the Unstable High-Low (uHL)/Low-High state (uLH) states, in contrast to their more stable counterparts termed High-Low (HL)/Low-High (LH) states (**Figure 1F and 1I**). The first capital letter in the abbreviation denotes the state of the molecule closer to the STM tip. The discrepancy between the stable and unstable configurations is likely resulting from the steric repulsion between molecules in proximity⁴⁹⁻⁵¹, which breaks the energy degeneracy of the four in-plane geometries of the molecule in the L state. The unstable states are much shorter-lived, typically appearing as intermediate steps during transitions between stable configurations. We primarily utilize the four stable configurations as the bases to fabricate a multi-level molecular switch.

To create a functional molecular switch, it is essential to reliably switch the molecule into a desired state on demand. At the experimental temperature of 5 K, spontaneous structural transitions do not occur for either monomers or dimers but can be driven by energetic tunneling electrons. For the monomers, the resulting configuration change can be tracked by monitoring changes between two tunneling current levels, with the feedback turned off and the STM tip positioned over the center of the pyrrolidine molecule. The occupation ratio of a state, defined as the average percentage of time a molecule remains in a specific configuration, varies with the sample bias, as shown in **Figure 2A**. When the bias is set below 20 mV, the tunneling electrons cannot trigger any structural transition. Between 30 and 40 mV,

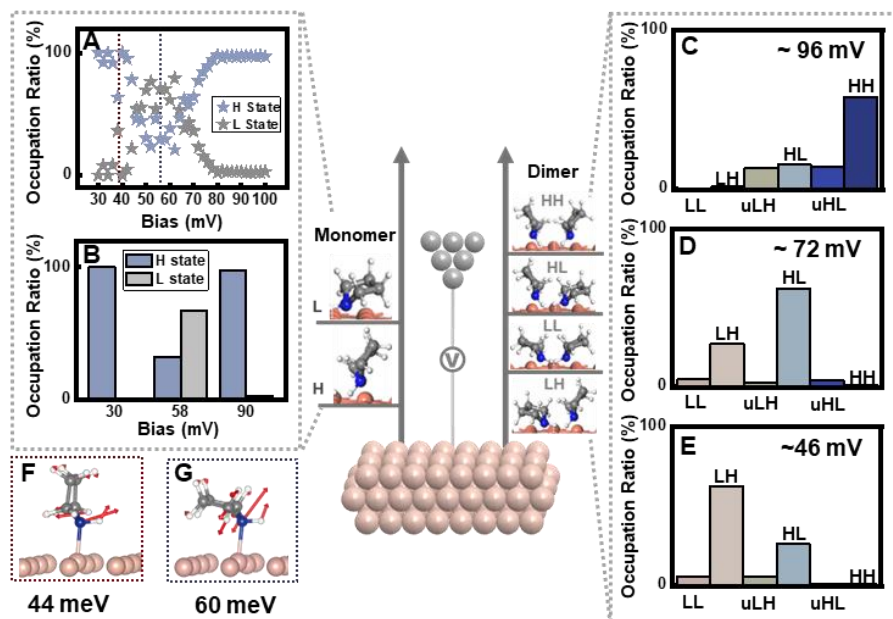


Figure 2. Occupation ratio of different molecular configuration as a function of sample bias. (A) Voltage-dependent occupation ratio the L and H states of a pyrrolidine monomer. (B) Statistic histogram of the occupation of monomer L and H states at 32/58/90 mV. (C)-(E) Occupation ratio of different dimer configurations (C)96 mV, (D)72 mV, and (E)46 mV. DFT simulations of the two vibrational modes at (F) 40 meV and (G) 58 meV, corresponding to the H-to-L and L-to-H transition thresholds in (A).

the molecule can be switched to and stays at the H state. Beyond this threshold, the occupation of the L state increases, reaching its peak at 60 mV. As the voltage increases further, a resurgence of the H state occurs, becoming the dominant state once again, as illustrated in **Figure 2B**.

The bias dependence of the H and L state occupation is closely linked to the dominant transition pathways excited by inelastic electron tunneling. To identify the nature of these pathways, we analyze the transition rate as a function of sample bias from current-time traces, which represent the probability that a tunneling electron at a given bias could trigger the transition. As shown in the **SI**, the transition rates display several distinct jumps at specific bias values, corresponding to the excitation of different vibrational modes that open new pathways for H-to-L or L-to-H transitions. By fitting the data using established formulas^{52, 53} (detailed in **SI Figure 1**), we determine the H-to-L transition thresholds to be approximately 44 meV and 78 meV, and the L-to-H thresholds to be around 60 meV and 74 meV. The competition between these transition pathways determines the overall H and L occupation of the molecule at different biases. When the bias is below 20 mV, the electron energy is insufficient to overcome the energy barrier between the L and H states, so the molecule remains in its initial

configuration. In the range between 30 to 40 mV, electrons occasionally trigger the L-to-H transition, switching the molecule to its more energetically favorable H state through some less probable pathways. Once the bias exceeds 44 mV, the excitation of a vibrational mode in the H state molecule (**Figure 2F**) opens an H-to-L transition channel, increasing the occupation of the L state. As the voltage approaches the L-to-H transition threshold of 60 mV, corresponding to a vibrational mode of the L state molecule (**Figure 2F**), a new L-to-H transition is activated, leading to a decrease in L state occupation beyond this point. Consequently, the molecular switch can be controlled by carefully tuning the energy of the tunneling electrons. For instance, the molecular configuration can be switched by applying a relatively high bias, then locked into that state by lowering the bias to below 20 mV. Therefore, identifying the specific bias at which the molecule preferentially occupies a desired configuration—such that it spends the majority of time in that state—is key to enabling consistent and reversible molecular switching.

To conveniently operate the dimer switch, it is crucial that transitions between all molecular configurations can be excited and monitored by tunneling electron injection at the same location. In the symmetric dimer we studied, we positioned the STM tip near one of the molecules, where we can identify all six distinct structural states by their different levels in the tunneling current. The tip's position is indicated by circles in **Figures 1E-J**. Notably, the transitions between these six states exhibit directionality depending on the position of the tip. Direct transitions between certain states, such as between the HH and LL states or the HL and LH states, have not been observed (**SI Figure 2**). These "forbidden" transitions all require simultaneous changes in both molecules, likely involving higher energy barriers or multiple electron excitations, making them less favorable.

Similar to the monomers, the occupation of different dimer states varies depending on the energy of tunneling electrons as illustrated in the **SI figure 3**. At bias between 30 and 40 mV, the dimer preferentially adopts the HH configuration, aligning with the behavior of the monomer where the H configuration is the more energetically preferable. As voltage increases, the molecules start to be excited into to L state, leading to the dominance of HL, LH, and LL states within the 40-75 mV range. The uHL and uLH states were only observed as the short intermediate step for the transition from HH to HL or LH states. The occupation ratios as a function of sample bias for both the HL and LH states exhibit a double-peak feature. In both states, two occupation maximums occur at approximately 45 meV and 70 meV. Although sharing the same peak energy, the relative occupation between these two states is

different. At approximately 45 mV, the dimer predominantly occupies the LH state, with an occupation ratio of about 63% (**Figure 2E**), whereas at around 72 mV, the HL state is favored with an occupation ratio of approximately 62% (**Figure 2D**). The LL state has a maximum occupation at around 60 mV, coinciding with the monomer case where the H state becomes preferable. As the voltage increases further, the HH state becomes dominant once again (Figure 2C). Note that even though the occupation of LL maximizes at around 60 mV, it is still comparable to HL, and LH states. However, the occupation of the other three stable states, HH, HL, and LH, can all be easily distinguished at different biases.

The HL and LH states are inherently symmetric, which is broken by the presence of the STM tip. **Figure 3** illustrates the effect of the tip-molecule distance on the occupation ratio of the HL and LH states of the dimer. When the tip is farther from the molecules, the dimer strongly favors the LH state at ~ 46 mV, with an occupation ratio of up to 75% (**Figures 3A and 3C**). As the tip moves closer to the sample, the proportion of the LH state steadily decreases at both 46 mV and 72 mV, with the HL state becoming increasingly dominant. At minimized tip-sample distance, the HL state predominates at 72

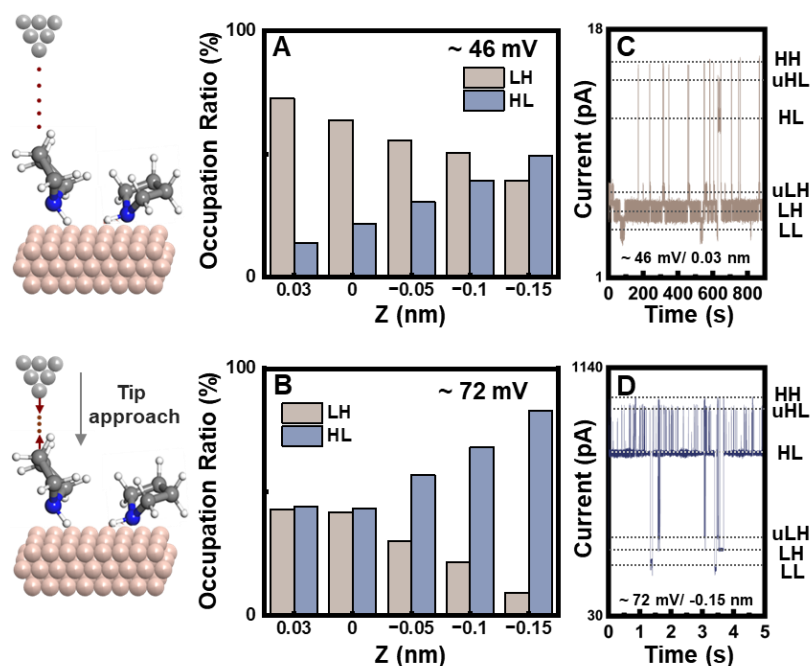


Figure 3. Alternation to the HL and HL state occupation by tip-molecule interaction. (A)-(B) Occupation ratio of the dimer HL and LH states at (A) 46 mV and (B) 72 mV at different tip molecule separation. The reference tunneling gap ($\Delta z=0$ nm) is set at 50 mV sample bias, 20 pA tunneling current. (C)-(D) The current traces taken at (C) $\Delta z=0.03$ nm and bias=46 mV, (D) $\Delta z=-0.15$ nm and bias=72 mV. Positive Δz refers to retracting the tip away from the molecule, negative Δz means approaching the tip toward the molecule.

mV, reaching an 83% occupancy (**Figures 3B and 3D**). Thus, by modulating the tip-molecule interaction, HL and LH states can be easily differentiated by their occupation at these two biases.

To understand the mechanism behind the operation of this multi-level dimer switch, three key factors must be considered: simultaneous excitation of both molecules in the dimer, tip-molecule interaction, and intermolecular couplings. If we model the dimer as two independent monomers excited simultaneously by tunneling electrons, the occupation of different dimer states can be represented as the product of the probabilities of the H and L states of each monomer at various bias voltages (SI Figure 4). Based on the monomer data in Figure 2A, the occupation probability of the L state can be approximated by a Gaussian function, $P(V)$, centered around 58 mV. Consequently, the probability of the H state is $1-P$. This leads to the LL state being expressed as P^2 , and the HL and LH states as $P(1-P)$. According to this model, the bias dependence of the HL and LH occupation is expected to exhibit a split double-peak feature, aligning with experimental observations (SI Figure 3), while the LL state retains a single peak centered around 58 mV. This naturally provides a mechanism to differentiate HL/LH and LL at different applied bias voltages.

To further tell between HL and LH, it is important to consider how the STM tip interacts differently with the two molecules. The tip exerts an attractive van der Waals force on the molecule directly beneath it, lowering the energy of the H configuration for that molecule. Therefore, as the tip approaches the molecule, the molecule closer to the tip prefers the H configuration, increasing the probability of the HL state over the LH at both 46 mV and 72 mV, as shown in **Figures 3A and 3B**. This allows this molecular switch to be easily switched to the HL state at 72 mV at a small tip-molecule separation.

However, there is an interesting discrepancy between the experimental observation and the simplified model described in Figure 4A: the LH state is much more favorable than the LH state at 46 mV even with a considerably large tip-molecule separation. If the HL and LH are solely differentiated by the tip-molecule van der Waals attraction, they should become less distinguishable when the tip is far away. Yet, as shown in **Figure 3A**, when the tip is retracted from the molecule, the LH state achieves an occupation ratio of up to 75%, while the LH state occupation is below 10%.

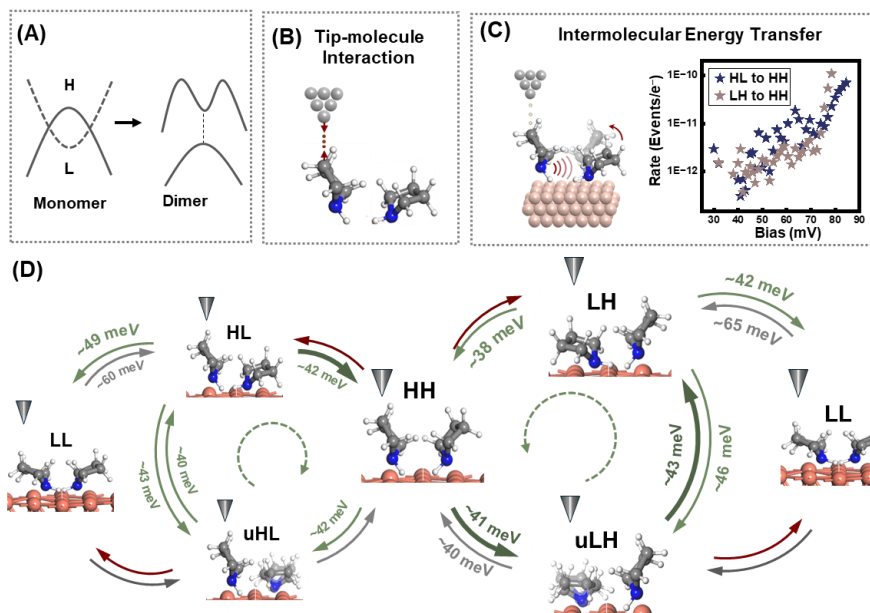


Figure 4. Schematic of reaction pathways of the dimer switching that can be activated by the inelastic tunneling electrons. (A) A simplified model estimating the dimer occupation ratio based on the occupation of H and L of a monomer. (B) Schematic diagram indicating how the interaction between the STM tip and the molecule underneath it is influencing the preference of difference dimmer configuration. (C) The HL/LH to HH transition rate as a function of bias. The lowest energy threshold is measured around 40 meV. (D) Schematic diagram of the directional transition between different dimer states and the corresponding energy thresholds extracted from the experimental measurement. The green arrows indicate that this transition can readily occur within the 40-60 mV range. Gray arrows indicate that the transition can occur but with a much lower chance. Red arrows indicate that the transition is rarely observed. The thicker green arrows indicate the most preferable transition path when bias is set around 46 meV, forming a directional transition pathway: HL → HH → uLH/uHL → LH.

To understand this discrepancy, we analyzed the directional transition between different dimer configurations at varying bias voltages (**SI Figures 5-8**). The identified transition thresholds between different states are shown in **Figure 4D**. When the bias is set between 40~50 mV, the dimer favors a unidirectional cyclic transition: HH-LH/HL-HH. Detailed discussion regarding how this directional transition is determined is included in the **SI**. Interestingly, it appears that the transition HL-HH-LH is much more favorable than HL-HH-HL, eventually leading to the dominant occupation of LH.

The directional transition from HL to LH is facilitated by interactions between the two molecules, which open new energy transfer channels and create distinct excitation pathways that are absent in the transitions of monomers. In monomers, the first transition pathway from the L to H is triggered by the excitation of a vibrational mode in the L state molecule at ~60 mV. However, when molecules form a

dimer, the transition from HL/LH to HH—also involving the transition of one molecule from L to H—shows two distinct threshold energies at ~ 40 meV and ~ 60 meV. The latter corresponds to the same pathway observed in the monomer L-to-H transition. The lower energy threshold, at ~ 40 meV, coincides with the vibrational mode of the H state molecule and was not present in the monomer transition.

This new lower-energy transition threshold suggests the existence of an energy transfer channel where the vibrationally excited H state molecule in the HL or LH configuration transfers energy to the neighboring L state molecule, prompting its transition from L to H. As shown in **Figure 4C**, the transition probability from HL to HH is significantly higher than that from LH. This discrepancy is likely related to the excitation probability of the H state vibration, which depends on the position of the STM tip. When the tip is positioned above the H state molecule of the dimer in the HL state, the cross-section for exciting the H state vibration is much greater than in the LH case, where the tip is positioned over the L state molecule. Additionally, since the H-to-L transition can be mediated by the same vibration, the HH-to-LH transition is also facilitated, during which the H-state molecule under the tip switches to the L state. These sequential preferential excitations create a directional LH-to-HL pathway when the bias is set to ~ 46 mV, even at a considerable tip-molecule separation, due to the continuous excitation of the vibration of the H state molecule.

Conclusion

In conclusion, our study presents an efficient and straightforward approach to on-demand control of a multi-state molecular switch utilizing a pyrrolidine dimer. The formation of a dimer introduces additional structural states without the involvement of complicated synthetic approaches. By positioning the STM at a location closer to one of the molecules in the dimer, we can not only monitor all different molecular structures but also break the energy degeneracy of some of these states via the tip-molecule interaction, allowing the differentiation of molecular configurations which are otherwise indistinguishable in energy. Intermolecular interactions introduce a new energy transfer channel, allowing the directional transfer between dimer configurations. By precisely adjusting the applied voltage and the tip-molecule distance, we have successfully presented a material candidate for a controllable multi-state molecular switch. This research elucidates the possibility of utilizing the fundamental molecule-environment interaction to manipulate the transition between molecular

conformations, paving the way for designing more complex and efficient molecular functional devices with artificial molecular clusters.

Acknowledgment

This work was supported by the United States National Science Foundation (NSF) under Grant No. CHE-2303936 (to Shaowei Li). The authors acknowledge the use of facilities and instrumentation supported by NSF through the UC San Diego Materials Research Science and Engineering Center (UCSD MRSEC) with Grant No. DMR-2011924.

Reference

1. Xu, X.; Gao, C.; Emusani, R.; Jia, C.; Xiang, D., Toward Practical Single-Molecule/Atom Switches. *Advanced Science* **2024/08/01**, *11* (29).
2. Xiang, D.; Wang, X.; Jia, C.; Lee, T.; Guo, X., Molecular-Scale Electronics: From Concept to Function. *Chemical Reviews* **2016**, *116* (7).
3. Chen, H.; Fraser Stoddart, J.; Chen, H.; Fraser Stoddart, J., From molecular to supramolecular electronics. *Nature Reviews Materials* **2021 6:9** **2021-04-01**, *6* (9).
4. Ratner, M.; Ratner, M., A brief history of molecular electronics. *Nature Nanotechnology* **2013 8:6** **2013-06-05**, *8* (6).
5. Murphy, C. J.; Sykes, E. C. H., Development of an Electrically Driven Molecular Motor. *The Chemical Record* **2014/10/01**, *14* (5).
6. J. Murphy, C.; C. Smith, Z.; Alex Pronschinski; A. Lewis, E.; L. Liriano, M.; Chloe Wong; J. Ivimey, C.; Mitchell Duffy; Wojciech Musial; Therrien, Andrew J.; Ill, S. W. T.; H. Sykes, E. C.; J. Murphy, C.; C. Smith, Z.; Alex Pronschinski; A. Lewis, E.; L. Liriano, M.; Chloe Wong; J. Ivimey, C.; Mitchell Duffy; Wojciech Musial; Therrien, Andrew J.; Ill, S. W. T.; H. Sykes, E. C., Ullmann coupling mediated assembly of an electrically driven altitudinal molecular rotor. *Physical Chemistry Chemical Physics* **2015/11/25**, *17* (47).
7. Perera, U. G. E.; Ample, F.; Kersell, H.; Zhang, Y.; Vives, G.; Echeverria, J.; Grisolia, M.; Rapenne, G.; Joachim, C.; Hla, S.-W.; Perera, U. G. E.; Ample, F.; Kersell, H.; Zhang, Y.; Vives, G.; Echeverria, J.; Grisolia, M.; Rapenne, G.; Joachim, C.; Hla, S.-W., Controlled clockwise and anticlockwise rotational switching of a molecular motor. *Nature Nanotechnology* **2012 8:1** **2012-12-23**, *8* (1).
8. Iancu, V.; Hla, S.-W.; Iancu, V.; Hla, S.-W., Realization of a four-step molecular switch in scanning tunneling microscope manipulation of single chlorophyll-a molecules. *Proceedings of the National Academy of Sciences* **2006-9-12**, *103* (37).
9. Zhang, Y.; Kersell, H.; Stefak, R.; Echeverria, J.; Iancu, V.; Perera, U. G. E.; Li, Y.; Deshpande, A.; Braun, K.-F.; Joachim, C.; Rapenne, G.; Hla, S.-W.; Zhang, Y.; Kersell, H.; Stefak, R.; Echeverria, J.; Iancu, V.; Perera, U. G. E.; Li, Y.; Deshpande, A.; Braun, K.-F.; Joachim, C.; Rapenne, G.; Hla, S.-W., Simultaneous and coordinated rotational switching of all molecular rotors in a network. *Nature Nanotechnology* **2016 11:8** **2016-05-09**, *11* (8).
10. Zhang, Y.; Calupitan, J. P.; Rojas, T.; Tumbleson, R.; Erbland, G.; Kammerer, C.; Ajayi, T. M.; Wang, S.; Curtiss, L. A.; Ngo, A. T.; Ulloa, S. E.; Rapenne, G.; Hla, S. W.; Zhang, Y.; Calupitan, J. P.; Rojas, T.; Tumbleson, R.; Erbland, G.; Kammerer, C.; Ajayi, T. M.; Wang, S.; Curtiss, L. A.; Ngo, A. T.; Ulloa, S. E.; Rapenne, G.; Hla, S. W., A chiral molecular propeller designed for unidirectional rotations on a surface. *Nature Communications* **2019 10:1** **2019-08-20**, *10* (1).
11. Huanyan Fu; Xin Zhu; Peihui Li; Mengmeng Li; Lan Yang; Chuancheng Jia; Xuefeng Guo; Huanyan Fu; Xin Zhu; Peihui Li; Mengmeng Li; Lan Yang; Chuancheng Jia; Xuefeng Guo, Recent progress in single-molecule transistors: their designs, mechanisms and applications. *Journal of Materials Chemistry C* **2022/02/17**, *10* (7).
12. Perrin, M. L.; Perrin, M. L.; Burzurí, E.; Burzurí, E.; Zant, H. S. J. v. d.; Zant, H. S. J. v. d., Single-molecule transistors. *Chemical Society Reviews* **2015/02/10**, *44* (4).

13. Martínez-Blanco, J.; Nacci, C.; Erwin, S. C.; Kanisawa, K.; Locane, E.; Thomas, M.; von Oppen, F.; Brouwer, P. W.; Fölsch, S.; Martínez-Blanco, J.; Nacci, C.; Erwin, S. C.; Kanisawa, K.; Locane, E.; Thomas, M.; von Oppen, F.; Brouwer, P. W.; Fölsch, S., Gating a single-molecule transistor with individual atoms. *Nature Physics* **2014** *11*:8 **2015-07-13**, *11* (8).
14. Serrate, D.; Ferriani, P.; Yoshida, Y.; Hla, S.-W.; Menzel, M.; von Bergmann, K.; Heinze, S.; Kubetzka, A.; Wiesendanger, R.; Serrate, D.; Ferriani, P.; Yoshida, Y.; Hla, S.-W.; Menzel, M.; von Bergmann, K.; Heinze, S.; Kubetzka, A.; Wiesendanger, R., Imaging and manipulating the spin direction of individual atoms. *Nature Nanotechnology* **2010** *5*:5 **2010-04-25**, *5* (5).
15. Coronado, E.; Coronado, E., Molecular magnetism: from chemical design to spin control in molecules, materials and devices. *Nature Reviews Materials* **2019** *5*:2 **2019-10-24**, *5* (2).
16. Torres, J. A. G.; Simpson, G. J.; Adams, C. J.; Früchtl, H. A.; Schaub, R., On-Demand Final State Control of a Surface-Bound Bistable Single Molecule Switch. *Nano Letters* **April 3**, **2018**, *18* (5).
17. Huang, T.; Zhao, J.; Feng, M.; Popov, A. A.; Yang, S.; Dunsch, L.; Petek, H., A molecular switch based on current-driven rotation of an encapsulated cluster within a fullerene cage. *Nano Lett* **2011**, *11* (12), 5327-32.
18. Bauer, A.; Maier, M.; Schosser, W. M.; Diegel, J.; Paschke, F.; Dedkov, Y.; Pauly, F.; Winter, R. F.; Fonin, M., Tip-Induced Inversion of the Chirality of a Molecule's Adsorption Potential Probed by the Switching Directionality. *Advanced Materials* **2020/03/01**, *32* (12).
19. Bauer, A.; Birk, T.; Paschke, F.; Fuhrberg, A.; Diegel, J.; Becherer, A.-K.; Vogelsang, L.; Maier, M.; Schosser, W. M.; Pauly, F.; Zilberberg, O.; Winter, R. F.; Fonin, M., Fully Reprogrammable 2D Array of Multistate Molecular Switching Units. *Advanced Materials* **2024**.
20. Dattler, D.; Fuks, G.; Heiser, J.; Moulin, E.; Perrot, A.; Yao, X.; Giuseppone, N., Design of Collective Motions from Synthetic Molecular Switches, Rotors, and Motors. *Chemical Reviews* **December 23, 2019**, *120* (1).
21. Sundus Erbas-Cakmak; Safacan Kolemen; C. Sedgwick, A.; Thorfinnur Gunnlaugsson; D. James, T.; Juyoung Yoon; U. Akkaya, E.; Sundus Erbas-Cakmak; Safacan Kolemen; C. Sedgwick, A.; Thorfinnur Gunnlaugsson; D. James, T.; Juyoung Yoon; U. Akkaya, E., Molecular logic gates: the past, present and future. *Chemical Society Reviews* **2018/04/03**, *47* (7).
22. Liu, L.; Liu, P.; Ga, L.; Ai, J., Advances in Applications of Molecular Logic Gates. *ACS Omega* **2021**, *6* (45), 30189-30204.
23. Gunther, K.; Grabicki, N.; Battistella, B.; Grubert, L.; Dumele, O., An All-Organic Photochemical Magnetic Switch with Bistable Spin States. *J Am Chem Soc* **2022**, *144* (19), 8707-8716.
24. Wasio, N. A.; Slough, D. P.; Smith, Z. C.; Ivimey, C. J.; Thomas III, S. W.; Lin, Y.-S.; Sykes, E. C. H.; Wasio, N. A.; Slough, D. P.; Smith, Z. C.; Ivimey, C. J.; Thomas III, S. W.; Lin, Y.-S.; Sykes, E. C. H., Correlated rotational switching in two-dimensional self-assembled molecular rotor arrays. *Nature Communications* **2017** *8*:1 **2017-07-04**, *8* (1).
25. Rośławska, A.; Kaiser, K.; Romeo, M.; Devaux, E.; Scheurer, F.; Berciaud, S.; Neuman, T.; Schull, G.; Rośławska, A.; Kaiser, K.; Romeo, M.; Devaux, E.; Scheurer, F.; Berciaud, S.; Neuman, T.; Schull, G., Submolecular-scale control of phototautomerization. *Nature Nanotechnology* **2024** *19*:6 **2024-02-27**, *19* (6).

26. Simpson, G. J.; Persson, M.; Grill, L.; Simpson, G. J.; Persson, M.; Grill, L., Adsorbate motors for unidirectional translation and transport. *Nature* **2023** *621*:7977 **2023-09-06**, 621 (7977).
27. Quintans, C. S.; Andrienko, D.; Domke, K. F.; Aravena, D.; Koo, S.; Díez-Pérez, I.; Aragonès, A. C.; Quintans, C. S.; Andrienko, D.; Domke, K. F.; Aravena, D.; Koo, S.; Díez-Pérez, I.; Aragonès, A. C., Tuning Single-Molecule Conductance by Controlled Electric Field-Induced trans-to-cis Isomerisation. *Applied Sciences* **2021**, Vol. 11, Page 3317 **2021-04-07**, 11 (8).
28. Lotze, C.; Luo, Y.; Corso, M.; Franke, K. J.; Haag, R.; Pascual, J. I.; Lotze, C.; Luo, Y.; Corso, M.; Franke, K. J.; Haag, R.; Pascual, J. I., Reversible electron-induced cis–trans isomerization mediated by intermolecular interactions. *Journal of Physics: Condensed Matter* **2012-09-11**, 24 (39).
29. Leary, E.; Roche, C.; Jiang, H.-W.; Grace, I.; González, M. T.; Rubio-Bollinger, G.; Romero-Muñiz, C.; Xiong, Y.; Al-Galiby, Q.; Noori, M.; Lebedeva, M. A.; Porfyrakis, K.; Agrait, N.; Hodgson, A.; Higgins, S. J.; Lambert, C. J.; Anderson, H. L.; Nichols, R. J., Detecting Mechanochemical Atropisomerization within an STM Break Junction. *Journal of the American Chemical Society* **January 4, 2018**, 140 (2).
30. Henningsen, N.; Rurali, R.; Franke, K. J.; Fernández-Torrente, I.; Pascual, J. I.; Henningsen, N.; Rurali, R.; Franke, K. J.; Fernández-Torrente, I.; Pascual, J. I., Trans to cis isomerization of an azobenzene derivative on a Cu(100) surface. *Applied Physics A* **2008** *93*:2 **2008-11-01**, 93 (2).
31. Bronner, C.; Schulze, G.; Franke, K. J.; Pascual, J. I.; Tegeder, P.; Bronner, C.; Schulze, G.; Franke, K. J.; Pascual, J. I.; Tegeder, P., Switching ability of nitro-spiropyran on Au(111): electronic structure changes as a sensitive probe during a ring-opening reaction. *Journal of Physics: Condensed Matter* **2011-11-16**, 23 (48).
32. Reeht, G.; Lotze, C.; Sysoiev, D.; Huhn, T.; Franke, K. J.; Reeht, G.; Lotze, C.; Sysoiev, D.; Huhn, T.; Franke, K. J., Disentangling electron- and electric-field-induced ring-closing reactions in a diarylethene derivative on Ag(1 1 1). *Journal of Physics: Condensed Matter* **2017-06-13**, 29 (29).
33. Kim, Y.; Motobayashi, K.; Frederiksen, T.; Ueba, H.; Kawai, M., Action spectroscopy for single-molecule reactions - Experiments and theory. *Progress in Surface Science* **2015**, 90 (2), 85-143.
34. Schied, M.; Prezzi, D.; Liu, D.; Kowarik, S.; Jacobson, P. A.; Corni, S.; Tour, J. M.; Grill, L., Chirality-Specific Unidirectional Rotation of Molecular Motors on Cu(111). *ACS Nano* **February 9, 2023**, 17 (4).
35. Ajayi, T. M.; Singh, V.; Latt, K. Z.; Sarkar, S.; Cheng, X.; Premarathna, S.; Dandu, N. K.; Wang, S.; Movahedifar, F.; Wieghold, S.; Shirato, N.; Rose, V.; Curtiss, L. A.; Ngo, A. T.; Masson, E.; Hla, S. W.; Ajayi, T. M.; Singh, V.; Latt, K. Z.; Sarkar, S.; Cheng, X.; Premarathna, S.; Dandu, N. K.; Wang, S.; Movahedifar, F.; Wieghold, S.; Shirato, N.; Rose, V.; Curtiss, L. A.; Ngo, A. T.; Masson, E.; Hla, S. W., Atomically precise control of rotational dynamics in charged rare-earth complexes on a metal surface. *Nature Communications* **2022** *13*:1 **2022-10-22**, 13 (1).
36. Auwärter, W.; Seufert, K.; Bischoff, F.; Eciya, D.; Vijayaraghavan, S.; Joshi, S.; Klappenberger, F.; Samudrala, N.; Barth, J. V.; Auwärter, W.; Seufert, K.; Bischoff, F.;

- Ecija, D.; Vijayaraghavan, S.; Joshi, S.; Klappenberger, F.; Samudrala, N.; Barth, J. V., A surface-anchored molecular four-level conductance switch based on single proton transfer. *Nature Nanotechnology* **2011** *7*:1 **2011-12-11**, 7(1).
37. Albrecht, F.; Fatayer, S.; Pozo, I.; Tavernelli, I.; Repp, J.; Peña, D.; Gross, L., Selectivity in single-molecule reactions by tip-induced redox chemistry. *Science* **2022-07-15**, 377(6603).
38. Mohn, F.; Repp, J.; Gross, L.; Meyer, G.; Dyer, M. S.; Persson, M., Reversible Bond Formation in a Gold-Atom--Organic-Molecule Complex as a Molecular Switch. *Physical Review Letters* **2010-12-28**, 105(26).
39. Stipe, B. C.; Rezaei, M. A.; Ho, W., Single-Molecule Vibrational Spectroscopy and Microscopy. *Science* **1998-6-12**, 280(5370).
40. Stipe, B. C.; Rezaei, M. A.; Ho, W., Inducing and Viewing the Rotational Motion of a Single Molecule. *Science* **1998-3-20**, 279(5358).
41. Okabayashi, N.; Peronio, A.; Paulsson, M.; Arai, T.; Giessibl, F. J.; Okabayashi, N.; Peronio, A.; Paulsson, M.; Arai, T.; Giessibl, F. J., Vibrations of a molecule in an external force field. *Proceedings of the National Academy of Sciences* **2018-5-1**, 115(18).
42. Ladenthin, J. N.; Frederiksen, T.; Persson, M.; Sharp, J. C.; Gawinkowski, S.; Waluk, J.; Kumagai, T.; Ladenthin, J. N.; Frederiksen, T.; Persson, M.; Sharp, J. C.; Gawinkowski, S.; Waluk, J.; Kumagai, T., Force-induced tautomerization in a single molecule. *Nature Chemistry* **2016 8:10** **2016-07-04**, 8(10).
43. Lu, H.-L.; Cao, Y.; Qi, J.; Bakker, A.; Strassert, C. A.; Lin, X.; Ernst, K.-H.; Du, S.; Fuchs, H.; Gao, H.-J., Modification of the Potential Landscape of Molecular Rotors on Au(111) by the Presence of an STM Tip. *Nano Letters* **July 2, 2018**, 18(8).
44. (李绍巍, S. L.; (陈思宇, S. C.; Li, J.; Wu, R.; Ho, W., Joint Space-Time Coherent Vibration Driven Conformational Transitions in a Single Molecule. *Physical Review Letters* **2017-10-26**, 119(17).
45. Single-Molecule Vibrations, Conformational Changes, and Electronic Conductivity of Five-Membered Heterocycles. *Journal of the American Chemical Society* **2001**, 123(41).
46. Lorente, N.; Rurali, R.; Tang, H.; Lorente, N.; Rurali, R.; Tang, H., Single-molecule manipulation and chemistry with the STM. *Journal of Physics: Condensed Matter* **2005-03-18**, 17(13).
47. Moresco, F.; Joachim, C.; Rieder, K. H., Manipulation of large molecules by low temperature STM. *Surface and Interface Analysis* **2004/02/01**, 36(2).
48. Eigler, D. M.; Schweizer, E. K.; Eigler, D. M.; Schweizer, E. K., Positioning single atoms with a scanning tunnelling microscope. *Nature* **1990 344:6266** **1990/04**, 344(6266).
49. Yang, H. J.; Trenary, M.; Kawai, M.; Kim, Y., Single-Molecule Dynamics in the Presence of Strong Intermolecular Interactions. *J Phys Chem Lett* **2016**, 7(21), 4369-4373.
50. Lee, J. G.; Ahner, J.; Yates, J. T., The adsorption conformation of chemisorbed pyridine on the Cu(110) surface. *The Journal of Chemical Physics* **2001**, 114(3), 1414-1419.
51. Dougherty, D. B.; Lee, J.; Yates, J. T., Role of conformation in the electronic properties of chemisorbed pyridine on Cu(110): An STM/STS study. *J Phys Chem B* **2006**, 110(24), 11991-11996.
52. Oh, J.; Lim, H.; Arafune, R.; Jung, J.; Kawai, M.; Kim, Y., Lateral Hopping of CO on Ag(110) by Multiple Overtone Excitation. *Physical Review Letters* **2016-02-02**, 116(5).
53. Ueba, H., Analysis of lateral hopping of a single CO molecule on Pd(110). *Physical Review B*

2012-07-24, 86 (3).